Bull. Astr. Soc. India (2003) **31**, 387–390

A Study of the Galactic Star Forming Region IRAS 02593+6016 / S 201 in Infrared and Radio Wavelengths

D.K. Ojha[1,*], S.K. Ghosh[1], V.K. Kulkarni[2], L. Testi[3], R.P. Verma[1], S. Vig[1]

[1]*Tata Institute of Fundamental Research, Mumbai (Bombay) - 400 005 (India)*
[2]*National Centre for Radio Astrophysics, Pune - 411007 (India)*
[3]*Osservatorio Astrofisico di Arcetri, Largo E. Fermi 5, 50125 Firenze (Italy)*

Abstract. We present infrared and radio observations of IRAS 02593+6016 / S 201 star forming region. A young star cluster is observed in this region, which contains different classes of young stellar objects. The near-infrared (NIR) color-color and color-magnitude diagrams are studied to discuss the nature of these sources. We have discovered the clumps of molecular hydrogen emission at 2.122 μm in the central region of S 201. These clumps are clearly seen along the diffuse emission in north-west direction from the main IRAS source, which are probably the obscured Herbig-Haro objects. High sensitivity and high resolution radio continuum images made with GMRT at 610 and 1280 MHz show an interesting arc-shaped structure due to the interaction between the HII region and the adjacent molecular cloud. The ionization front at the interface between the HII region and the molecular cloud is clearly seen by comparing the radio, molecular hydrogen and Brγ images.

1. Observations

tions and data reduction

HK) NIR observations were carried out on 23rd December 2000 using the
a (ARNICA) mounted on the 1.5m/f20 infrared telescope TIRGO. ARNICA
NICMOS3 256×256 HgCdTe detector. The plate scale at TIRGO was 0.96

he target field in the three standard J (1.25 μm, $\Delta\lambda$ = 0.3 μm), H (1.6 μm,
1 K (2.2 μm, $\Delta\lambda$ = 0.4 μm) broad-band filters. A large number of dithered

es.in

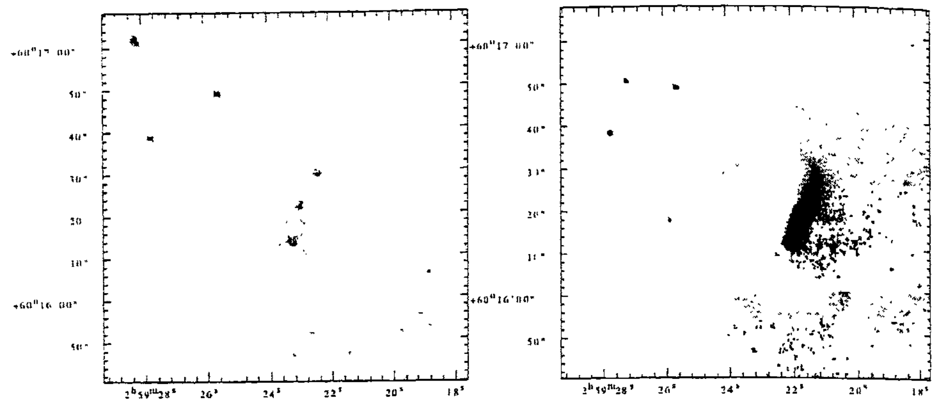

Figure 1. (left) H_2 line (continuum subtracted) and (right) continuum subtracted Brγ images of S 201 region. North is the top and east to the left.

sky frames were obtained (by shifting the telescope a few arcmin off the source in north-west-south-east directions) in all the filters for sky subtraction and for making flat frames. The total integration times on-target were 24 s, 24 s, and 60 s, respectively, in the J, H, and K bandpasses. The photometric calibration was obtained by observing the standard stars AS03 & AS09 (Hunt et al. 1998) in all three bands.

The images through narrow-band filters including the molecular hydrogen (H_2 $v = 1 - 0$ $S(1)$) transition (2.122 μm, FWHM = 0.032 μm), the Brγ line (2.169 μm, FWHM = 0.035 μm), and continuum K (Kcont at 2.275 μm, FWHM = 0.039 μm), were obtained on 13th Nov., 2002 at 3.58m TNG telescope at La Palma. The total integration time was of 90 s in all three filters. The images were analysed in a similar process as those from TIRGO. The continuum subtracted images were made after aligning and PSF matching. Fig. 1 shows the H_2 continuum subtracted (reveal the pure H_2 line emission), and Brγ continuum subtracted images.

1.2 Radio observations

The GMRT observations of S 201 were carried out at two frequency bands, viz., 610 & 1280 MHz on 04th January, 2002 and 28th September, 2002, respectively. The sources 3C48 and 3C147 were used as the primary flux calibrators for 610 & 1280 MHz observations, respectively, while the source 0432+416 was used as a secondary calibrator for both observations. The GMRT antennas and their configurations are discussed in detail by Swarup et al. (1991). Data reduction was done in classic AIPS. Bad data (dead antennas, inteference, spikes, etc.) were identified and flagged using UVFLG & TVFLG. Images of the field were formed by Fourier inversion and cleaning (IMAGR). The initial images were improved by self-calibration (CALIB) in both phase and amplitude. The radio continuum images have a resolution of $4''.5 \times 2''.5$ at 1280 MHz, and

8″.7×5″.7 at 610 MHz. The images have an rms of 42 μJy beam^{-1} at 1280 MHz, and 47 μJy beam^{-1} at 610 MHz.

2. Results

Fig. 2 shows the J-H/H-K color-color and K/H-K color-magnitude diagrams of the sources in S 201 region. In Fig. 2 (left), the solid curve is the locus of points corresponding to unreddened main sequence stars (Koornneef 1983). The two dashed lines are parallel to the reddening vector with magnitude of A_V = 25 mag. They form the reddening band (drawn from the base and tip of the unreddened main sequence) and bound the region in which stars with normal photosphere fall. Similarly, in Fig. 2 (right), the soild line represents the locus of unreddened main sequence stars and the dashed arrow shows the direction and magnitude of the reddening vector. The stars on the right side are mostly young stellar objects (YSOs) of different classes (Lada & Adams 1992; Lada et al. 1993; Gomez et al. 1994).

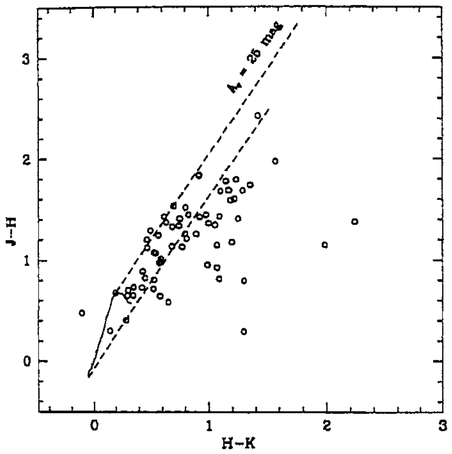

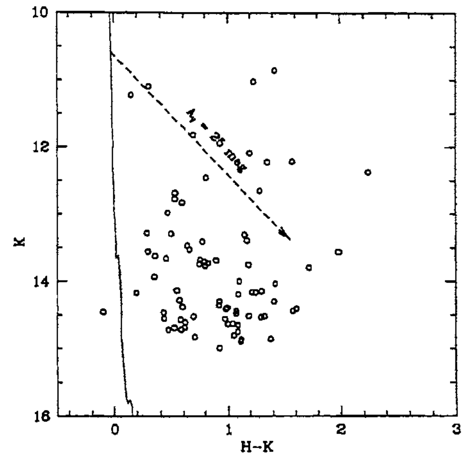

Figure 2. (left) Color-color diagram of the sources in S 201 region. The solid line represents unreddened main-sequence stars and the dashed lines are parallel to the reddening vector with magnitude of A_V = 25 mag. (right) Color-magnitude diagram of the same sources as in the left figure.

The quadrupole transition ($v = 1 - 0\ S(1)$) of molecular hydrogen at 2.122 μm is an excellent tracer of shock emission. We have probably found the clumps of H_2 emission. These clumps are clearly seen along the diffuse emission along north-west direction (shown by arrows in Fig. 1 (left)). These clumps of H_2 detected in emission could be HH objects.

The Brγ image displays a morphology very similar to the radio continuum map (Figs. 1 & 3), with a cometary shape, and a peak which is essentially coincident with the radio continuum one. The similar morphology between the two maps suggests that there are no steep extinction

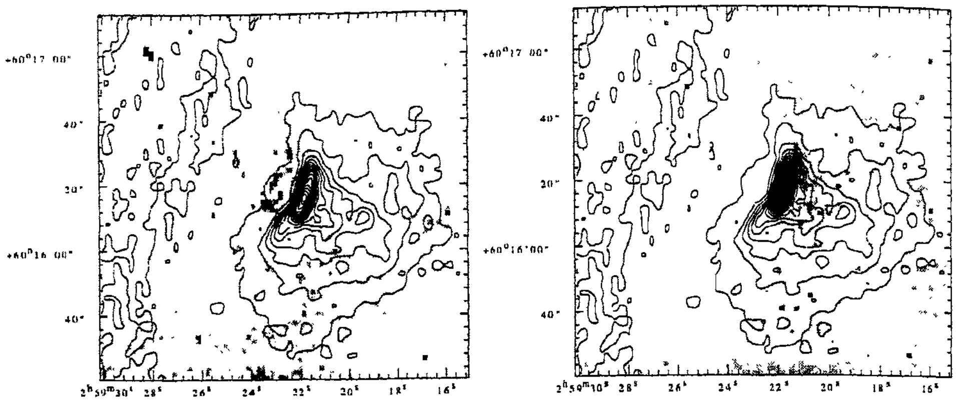

Figure 3. (left) Continuum subtracted H2 image of the IRAS 02593+6016 / S 201 region. (right) Continuum subtracted Brγ image. The contour plot shows the GMRT 1280 MHz radio continuum emission.

gradients across the region. The ionization front at the interface between the HII region and the molecular cloud are clearly seen by comparing the radio, molecular hydrogen and Brγ images (Figs. 1 & 3).

References

Gomez, M., Kenyon, S. J, Hartmann, L. 1994, *Astron. J.*, **107**, 1850.
Hunt, L. K., Mannucci, F, Testi, L., et al. 1998, *Astron. J.*, **115**, 2594.
Koornneef, J. 1983, *Astron. & Astrophys.*, **128**, 84.
Lada, C. J., Adams, F. C. 1992, *Astrophys. J*, **393**, 278.
Lada, C. J., Young, E. T., Greene, T. P. 1993, *Astrophys. J*, **408**, 471.
Swarup, G., Ananthakrishnan, S., Kapahi, V. K., et al. 1991, *Current Science*, **60**, 95.